

# PHYSICO-CHEMICAL INTERACTION IN THE BiSI–BiSeI SYSTEM

Abbas Qurbanov<sup>1</sup>, Elvin Ahmadov<sup>2,3</sup>, Isfandiyar Alverdiyev<sup>1</sup>, Yasin Jafarov<sup>4</sup>

<sup>1</sup>Ganja State University, Ganja, Azerbaijan

<sup>2</sup>Institute of Catalysis and Inorganic Chemistry, Baku, Azerbaijan

<sup>3</sup>Azerbaijan State University of Economics (UNEC), Baku, Azerbaijan

<sup>4</sup>Baku State University, Baku, Azerbaijan

Received: 15 november 2024

Accepted: 06 december 2024

Published: 24 december 2024

---

The phase diagram of the BiSI–BiSeI system was constructed based on the results of the DTA and XRD measurements. It was determined that it is stable in subsolidus and forms continuous solid solutions between the BiSI and BiSeI compounds. In general, the system is non-quasibinary due to the incongruent melting character of primary compounds. The lattice parameters *a*-, *b*-, and *c*- increase linearly within the homogeneity area of the  $\gamma$ -phase according to Vegard's rule. Obtained new solid solutions are of interest as optic and high-performance semiconductor materials.

**Keywords:** BiSI–BiSeI system, phase diagram, solid solutions, layered structure.

---

## INTRODUCTION

In recent years, the discovery of 3D Rashba spin splitting and topological insulator properties, along with thermoelectric, photovoltaic, optical properties, in layered stibium and bismuth chalcogenides and chalcogenides has significantly increased interest in these materials. These innovative materials, which exhibit unique physical properties, are widely utilized in electronics and technology for the creation of next-generation devices and systems that are energy-efficient, environmentally friendly, and economically viable [1-9].

BiTeI, BiSI and BiSeI chalcogenides exhibit significant spin-splitting effects that enable efficient spin current generation, and potential as high-performance semiconductors with tunable band gaps, which makes them suitable for optoelectronic and spintronic applications [7,10-14]. Furthermore, layered chalcogenides exhibit anisotropic electronic structures, band alignments, and optical properties, which leads to an increase in absorption coefficients in the near and visible infrared spectra and also in charge carrier mobility within the lattice. Due to these properties, they are considered perspective materials for photovoltaic efficiencies and light-harvesting applications.

One of the convenient ways to optimize the superior functional properties of  $B^V X Hal$  ( $B^V$ -As,Sb,Bi, X-S,Se,Te, Hal-Cl,Br,I) type compounds is to obtain new multicomponent non-stoichiometric phases of variable composition by studying phase equilibrium in relevant systems. Because in such phases it is possible to change the composition at large intervals, which opens up opportunities for purposeful change of properties [15-19].

In this work, the character of the physico-chemical interaction in the  $Bi_2S_3$ - $BiI_3$ - $Bi_2Se_3$  quasi-ternary system along the BiSI–BiSeI cross-section was studied and the phase diagram of the cross-section was constructed.

The primary compounds of title system have been studied in detail. The BiSI compound melts incongruently by decomposition according to the peritectic reaction at 808 K [20,21]. It crystallizes in the orthorhombic crystal structure with space group *Pnma*:  $a=8.529$ ;

$b=4.172$ ;  $c=10.177$  Å [22]. Another initial compound, BiSeI also melts by decomposition due to the peritectic reaction at 818 K [23]. It crystallizes in the SbSI-type orthorhombic crystal lattice with space group Pnma:  $a=8.697(2)$ ;  $b=4.221(1)$ ;  $c=10.574(2)$  Å;  $z = 4$  [24].

## EXPERIMENTAL

### Materials preparation and synthesis

The BiSI, BiSeI compounds and  $\text{BiS}_x\text{Se}_{1-x}\text{I}$  solid solutions were synthesized by co-melting of high purity elements (99.999% by weight) purchased from Alfa Aesar. The syntheses were carried out in evacuated sealed ampoules (residual pressure of  $10^{-3}$  Pa) using a two-zone inclined furnace considering the high vapor pressure of elemental iodine and sulfur, by a specially designed methodology. The temperature of the upper "cold" zone (440 K) was slightly lower than the boiling point of iodine (457.5 K) [25,26], while the temperature of the lower "hot" zone was 30-50 K higher than the melting point of the synthesized compound. In the specified regime, the ampoules were held until the complete disappearance of iodine vapors in the "cold" zone. Then, the ampoule was fully inserted into the "hot" zone, and the temperature was lowered to 770 K, which is slightly below the peritectic decomposition temperatures of BiSI (808 K) and BiSeI (818 K), and maintained for an additional 5-6 hours. By recording the DTA curves of the samples obtained in this way, it was established that they contained  $\text{BiI}_3$ . Considering this, in the next stage, the samples were ground, pressed into tablet form, and annealed at 750 K for 300 hours to achieve complete homogenization. Figure 1 presents the DTA heating curves of the BiSI sample before (Fig. 1a) and after (Fig. 1b) annealing. As can be seen, the thermal effect at 668 K, associated with the melting of  $\text{BiI}_3$  (or more precisely, the eutectic near  $\text{BiI}_3$  in the  $\text{Bi}_2\text{S}_3 - \text{BiI}_3$  system [21]), is absent in the DTA curve of the sample after annealing for 300 hours.

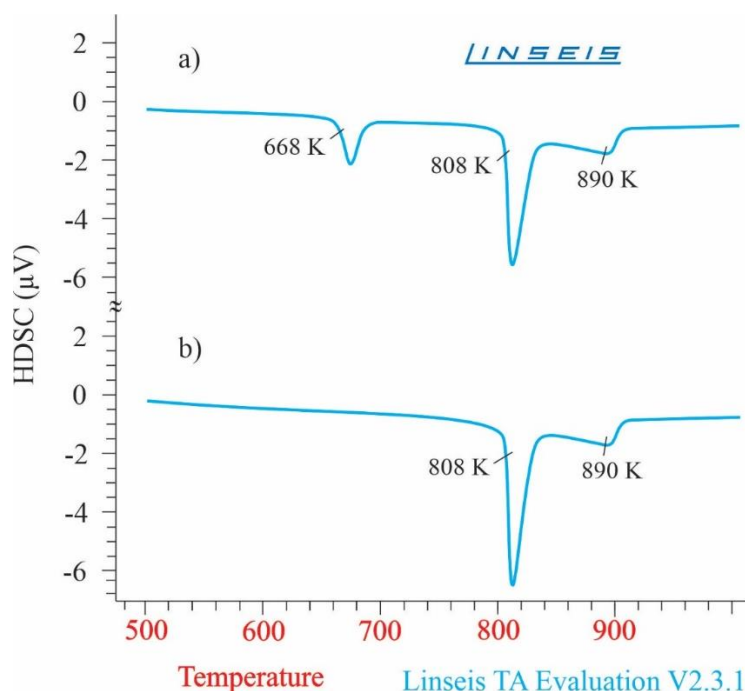


**Fig. 1.** DTA curves of the BiSI compound: (a) before thermal treatment and (b) after thermal treatment

Two sets of intermediate alloys of different compositions (0.5 g each) of the BiSI -BiSeI system were prepared in a vacuum by co-melting the stoichiometric amounts of preliminarily synthesized and identified ternary compounds. The samples were annealed at 750 K for 600 hours to bring them closer to the equilibrium state.

### Methods

The obtained samples were analyzed using differential thermal analysis (DTA) and X-ray diffraction (XRD) techniques. "Netzsch 404 F1 Pegasus system" differential scanning calorimeter and a multichannel thermal analyzer based on the electronic "TC-08 thermocouple data logger" (speed of heating 7-10 K/min) were used in DTA measurements. Bruker D2 PHASER diffractometer at the scanning range of  $2\theta=5\div75$  ( $\text{CuK}\alpha$  radiation) was used for recording of XRD patterns. The calculation of the lattice parameters was carried out by using the TOPAS 4.2

## RESULTS AND DISCUSSION.

The powder diffraction patterns of some homogenized  $\text{BiS}_x\text{Se}_{1-x}\text{I}$  alloys are presented in Figure 2. They clearly show that all intermediate composition samples exhibit qualitatively identical reflection lines with the initial BiSI and BiSeI compounds. We determined that each diffraction peak is indexed in the orthorhombic syngony with space group Pnma, which confirms the single-phase of the samples. Additionally, the increasing values of  $x$  are associated with a slight shift of the peaks toward higher angles, which arises due to differences in the ionic radii between S and Se, a characteristic feature of substitutional solid solutions.

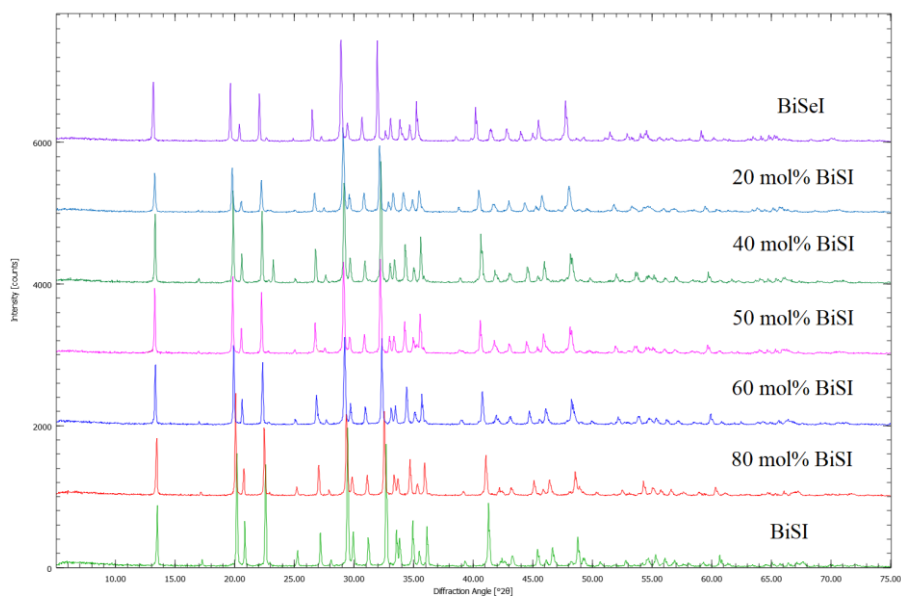


Fig. 2. PXRD patterns for different alloys of the BiSI-BiSeI system

Table 1 presents the DTA data of homogenized samples obtained by heating in vacuum-sealed ampoules, while Figure 3 shows the T-x phase diagram of the system constructed based on these data. In interpreting the DTA results, we considered the incongruent melting behavior of the initial compounds and the presence of a continuous series of solid solutions in the subsolidus area of the system.

Table 1. DTA results for BiSI-BiSeI system

Composition, mol%	BiSeI	Thermal effects, K
0 (BiSI)		808; 890
10		809; 883
20		810.5; 875
30		812; 864
40		813; 856
50		813.7; 847
60		815; 836
70		815.5; 829
80		816; 822
90		817.5; 827
100 (BiSeI)		818; 830

As seen from the data in Table 1 and Figure 3, the liquidus curve passes through a minimum point at a composition of approximately 80 mol% BiSel, in agreement with literature data on phase equilibria in the  $\text{Bi}_2\text{S}_3\text{--BiI}_3$  [21] and  $\text{Bi}_2\text{Se}_3\text{--BiI}_3$  [23] systems. During the crystallization of the incongruently melting compound BiSI, initially  $\text{Bi}_{19}\text{S}_{27}\text{I}_3$  crystals precipitate from the liquid at 890 K, and then a peritectic reaction occurs at 808K:



In the case of BiSel,  $\text{Bi}_2\text{Se}_3$  crystals first precipitate from the liquid at 830K, and then a peritectic reaction occurs at 818K:



Taking this into account, it can be assumed that in the BiSI–BiSel system, for compositions  $\leq 80$  mol% BiSel (to the left of the minimum point), the liquidus corresponds to the primary crystallization of solid solutions based on  $\text{Bi}_{19}\text{S}_{27}\text{I}_3$  ( $\alpha$ -phase), while for compositions  $\geq 80$  mol% BiSel (to the right of the minimum point), it corresponds to solid solutions based on  $\text{Bi}_2\text{Se}_3$  ( $\beta$ -phase).

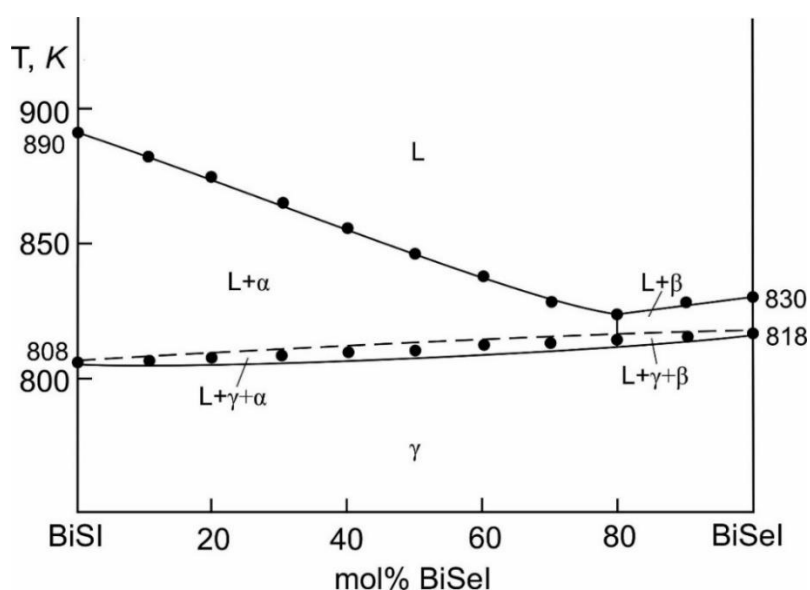


**Fig. 3.** BiSI–BiSel isopleth section

Furthermore, it can be assumed that in the corresponding composition areas, the crystallization of  $\text{BiS}_{1-x}\text{Se}_x\text{I}$  solid solutions ( $\gamma$ -phase) occurs through peritectic reactions respectively:



Since these reactions, according to the phase rule, must be monovariant, despite the presence of clear peaks on the DTA curves (Figure 4, endothermic effects at 810.5 and 815 K) corresponding to these processes, it is evident that they proceed monovariantly within narrow temperature ranges. Therefore, in Figure 3, the pre-phase areas  $\text{L} + \alpha + \gamma$  and  $\text{L} + \beta + \gamma$  are delineated by dashed lines.

We are aware that the phase diagram presented by us near the composition of 80 mol% BiSel is simplified. A more accurate depiction of phase equilibria can be established through a comprehensive study of the  $\text{Bi}_2\text{S}_3\text{--Bi}_2\text{Se}_3\text{--BiI}_3$  system in entire composition. Thus, the system under consideration is non-quasibinary due to the incongruent melting character of the BiSI and BiSel compounds. In the above peritectic reactions, the primary liquid and crystalline phases are completely consumed and a homogeneous  $\gamma$ -phase is obtained since the nominal compositions of the samples lie in the BiSI–BiSel area, where these solid solutions are formed.

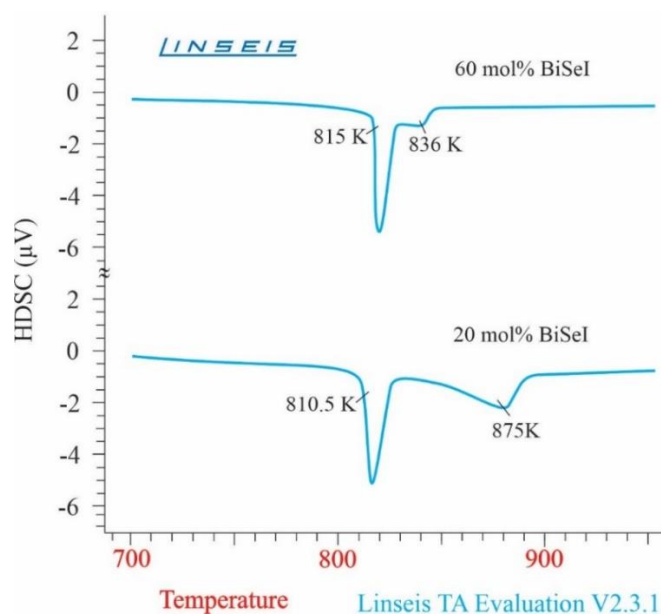


**Fig. 4.** DTA curves of some alloys of the BiSI–BiSeI system

The Orthorhombic (Pnma) crystal lattice constants for the  $\gamma$ -solid solutions were calculated using Topas V 4.2 computer software (Table 2) from the PXRD patterns given in Figure 2.

**Table 2.** Crystal lattice constants for the  $\text{BiS}_x\text{Se}_{1-x}\text{I}$  alloys.

Phase, mol%	Lattice parameters, Å		
	<i>a</i>	<i>b</i>	<i>c</i>
100 (BiSI)	8.5090	4.1765	10.2557
80 ( $\gamma$ )	8.5542	4.1841	10.3299
60 ( $\gamma$ )	8.5915	4.1938	10.3971
50 ( $\gamma$ )	8.6297	4.1973	10.4225
40 ( $\gamma$ )	8.6353	4.2011	10.4551
20 ( $\gamma$ )	8.6652	4.2128	10.5140
0 (BiSeI)	8.7044	4.2209	10.5807

It is clearly seen from the concentration dependence graph of lattice constants for  $\text{BiS}_x\text{Se}_{1-x}\text{I}$  solid solutions given in Figure 5 that *a*-, *b*-, and *c*- parameters increase as a linear function of composition within the homogeneity area of the  $\gamma$ -phase according to Vegard's rule.

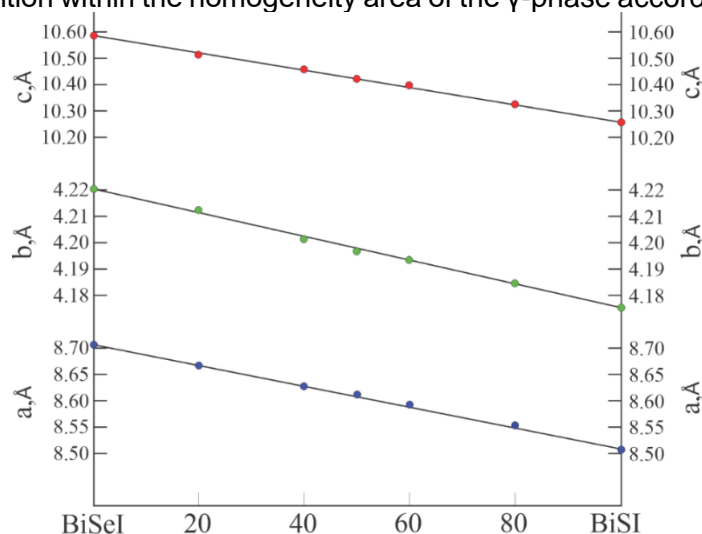


**Fig. 5.** Concentration dependence of the lattice constants for the  $\gamma$ -solid solutions.

## CONCLUSION

In this paper, physico-chemical interaction in the BiSI–BiSel system was studied over the entire concentration range and a phase diagram was constructed by using DTA and XRD methods. The system is non-quasibinary, but it is stable in subsolidus and characterized by the formation of continuous solid solutions between primary compounds. The lattice parameters *a*-, *b*-, and *c*- increase linearly within the homogeneity area of the  $\gamma$ -phase according to Vegard's rule. Obtained new solid solutions between the initial compounds are of interest as potential optic and high-performance semiconductor materials.

## REFERENCES

- [1] Vieira, E.M.F., Figueira, J., Pires, A.L., Grilo, J., Silva, M.F., Pereira, A.M., Goncalves, L.M. Enhanced thermoelectric properties of  $\text{Sb}_2\text{Te}_3$  and  $\text{Bi}_2\text{Te}_3$  films for flexible thermal sensors. *J. Alloy. Compd.* 2019, 774, pp. 1102–1116, <https://doi.org/10.1016/j.jallcom.2018.09.324>
- [2] Narendra, N., Kim, K.W. Toward enhanced thermoelectric effects in  $\text{Bi}_2\text{Te}_3/\text{Sb}_2\text{Te}_3$  heterostructures. *Semicond. Sci. Technol.* 2017, 32, pp. 035005, <https://doi.org/10.1088/1361-6641/aa539d>
- [3] Li X., Lou C., Li X., Zhang Y., Liu Z., Yin B.  $\text{Bi}_2\text{Te}_3/\text{Sb}_2\text{Te}_3$  thermophotovoltaic cells for low temperature infrared radiation. *J. Phys. D: Appl. Phys.* 2020, 53, pp. 035102–035107, <https://doi.org/10.1088/1361-6463/ab4edb>
- [4] Zhang W., Yu R., Zhang H.J., Dai X., Fang Z. First-principles studies of the three-dimensional strong topological insulators  $\text{Bi}_2\text{Te}_3$ ,  $\text{Bi}_2\text{Se}_3$  and  $\text{Sb}_2\text{Te}_3$ . *New. J. Phys.* 2010, 12, pp. 065013–065027, <https://doi.org/10.1088/1367-2630/12/6/065013>
- [5] Koc H., Palaz S., Mamedov A.M., Ozbay E. Optical, electronic, and elastic properties of some  $\text{A}_5\text{B}_6\text{C}_7$  ferroelectrics (A=Sb, Bi; B=Te, S, Se; C=I, Br, Cl): First principle calculation. *Ferroelectrics*, 2017, 511, pp. 22–34, <http://dx.doi.org/10.1080/00150193.2017.1332967>
- [6] Babanly M.B., Chulkov E.V., Aliev Z.S., Shevelkov A.V., Amiraslanov I.R. Phase Diagrams in Materials Science of Topological Insulators Based on Metal Chalcogenides. *Rus. J. I. Chem.* 2017, 62(13), pp. 1703–1729, <https://doi.org/10.1134/S0036023617130034>
- [7] Landolt G., Eremeev S.V., Koroteev Y.M., Slomski B., Muff S., Neupert T., Kobayashi M., Strocov V.N., Schmitt T., Aliev Z.S., Babanly M.B., Amiraslanov I.R., Chulkov E.V., Osterwalder J. and Dil J.H. Disentanglement of Surface and Bulk Rashba Spin Splittings in Noncentrosymmetric BiTeI. *Rew. Phys. Rev. Letters.* 2012, 109(11), pp. 116403, <https://doi.org/10.1103/PhysRevLett.109.116403>
- [8] Ishizaka K., Bahramy M.S., Murakawa H., Sakano M., Shimojima T., Sonobe T., Koizumi K., Shin S., Miyahara H., Kimura A., Miyamoto K., Okuda T., Namatame H., Taniguchi M., Arita R., Nagaosa N., Kobayashi K., Murakami Y., Kumai R., Kaneko Y., Onose Y. and Tokura Y. Giant Rashba-type spin splitting in bulk BiTeI. *Nat. Mater.* 2011, 10(7), pp. 521–526, <https://doi.org/10.1038/nmat3051>
- [9] Holtgrewe, K., Mahatha, S.K., Sheverdyayeva, P.M. Moras, P., Flammini, R., Colonna, S., Ronci, F., Papagno, M., Barla, A., Petaccia, L., Aliev, Z.S., Babanly, M.B., Chulkov, E.V., Sanna, S., Hogan, C. and Carbone, C. Topologization of  $\beta$ -antimonene on  $\text{Bi}_2\text{Se}_3$  via proximity effects. *Sci Rep.* 2020, 10, pp. 14619, <https://doi.org/10.1038/s41598-020-71624-4>
- [10] Ganose, A.M., Butler, K.T., Walsh, A. and Scanlon, D.O. Relativistic electronic structure and band alignment of BiSI and BiSel: candidate photovoltaic materials. *J. Mater. Chem. A.* 2016, 4, pp. 2060–2068, <https://doi.org/10.1039/C5TA09612J>
- [11] Audzijonis, A., Zaltauskas, R., Sereika, R., Zigas, L. and Reza, A. Electronic structure and optical properties of BiSI crystal // *J. Phys. Chem. Solids.* 2010, 71, pp. 884–891, <https://doi.org/10.1016/j.jpcs.2010.03.042>
- [12] Bahramy, M.S., Yang, B.J., Arita, R. and Nagaosa N. Emergence of non-centrosymmetric topological insulating phase in BiTeI under pressure. *Nat Commun.* 2012, 3, pp. 679, <https://doi.org/10.1038/ncomms1679>

- [13] Genep, D.V., Maiti, S., Graf, D., Tozer, S.W., Martin, C., Berger, H., Maslov, and D.L., Hamlin, J.J. Pressure tuning the Fermi level through the Dirac point of giant Rashba semiconductor BiTe. *J. Phys.: Condens Matter.* 2014, 26, pp. 342202, <https://doi.org/10.1088/0953-8984/26/34/342202>
- [14] Shi, H., Ming, W. and Du, M.H. Bismuth chalcogenides and oxyhalides as optoelectronic materials. *Phys. Rev. B.* 2016, 93, pp. 104108, <https://doi.org/10.1103/PhysRevB.93.104108>
- [15] Ahmadov, E.J., Orujlu, E.N., Babanly, D.M., Mammadov, D.A., Alizade, E.H., Mamedova, I.A., Abdullayev, N.A., Mamedov, N.T. and Babanly, M.B. Phase equilibria of the  $\text{Sb}_2\text{Te}_3+2\text{BiI}_3 \leftrightarrow \text{Bi}_2\text{Te}_3+2\text{SbI}_3$  reciprocal system: Synthesis and characterization of the cation-substituted  $\text{Bi}_{1-x}\text{Sb}_x\text{Te}$  solid solutions. *J. Alloys Compd.* 2022, 929, pp. 167388. <https://doi.org/10.1016/j.jallcom.2022.167388>
- [16] Aliev, Z.S., Ahmadov, E.C., Babanly, D.M., Amiraslanov, I.R. and Babanly, M.B. The  $\text{Bi}_2\text{Se}_3\text{-Bi}_2\text{Te}_3\text{-BiI}_3$  system: synthesis and characterization of the  $\text{BiTe}_{1-x}\text{Se}_x\text{I}$  solid solutions. *Calphad.* 2019, 66, pp. 101650, <https://doi.org/10.1016/j.calphad.2019.101650>
- [17] Ahmadov, E.J., Aliev, Z.S., Babanly, D.M., Imamaliyeva, S.Z., Gasymov, V.A. and Babanly, M.B. The Quasi-Ternary system  $\text{Bi}_2\text{S}_3\text{-Bi}_2\text{Te}_3\text{-BiI}_3$ . *Russ. J. Inorg. Chem.* 2021, 66, pp. 538–549, <https://doi.org/10.1134/S0036023621040021>
- [18] Ahmadov, E.J., Physico-chemical interaction in the  $\text{BiSI-BiTe}$  system. *Az. Chem. J.* 2020, 1, pp. 36–40.
- [19] Ahmadov, E.J., Babanly, D.M., Aliyev, Z.S. and Zlamanov, V.P. Phase equilibria in the system  $\text{SbTe-BiTe}$  // *NMC&A.* 2019, 3(2), pp. 87-93.
- [20] Aliev, Z.S., Musayeva, S.S., Jafarli, F.Y., Amiraslanov, I.R., Shevelkov, A.V. and Babanly, M.B. et al. The phase equilibria in the  $\text{Bi-S-I}$  ternary system and thermodynamic properties of the  $\text{BiSI}$  and  $\text{Bi}_{19}\text{S}_{27}\text{I}_3$  ternary compounds. *J. Alloys Compd.* 2014, 610, pp. 522-528, <https://doi.org/10.1016/j.jallcom.2014.05.015>
- [21] Ryazantsev, T.A., Varekha, L.M., Popovkin, B.A. and Novoselova, A.V.  $\text{P-T-x}$  phase diagram of the  $\text{BiI}_3\text{-Bi}_2\text{S}_3$  system. *Inorg. Mater.* 1970, 6, pp. 1175-1179.
- [22] Miede, G. and Kupcik, V. Die Kristallstruktur des  $\text{Bi}(\text{Bi}_2\text{S}_3)_9\text{J}_3$ . *Naturwissenschaften.* 1971, 58, pp. 219.
- [23] Petasch, U., Gobel, H. and Oppermann, H. Investigations on the pseudobinary system  $\text{Bi}_2\text{Se}_3/\text{BiI}_3$ . *Z. Anorg. Allg. Chem.* 1996, 624, pp. 1767-1769.
- [24] Braun, T.P. and DiSalvo, F.J. Bismuth selenide iodide. *Acta Crystallogr C.* 2000, 56(1), pp. e1-e2, <https://doi.org/10.1107/S0108270199016017>
- [25] Leenson, I.A. Sublimation of Iodine at Various Pressures: Multipurpose Experiments in Inorganic and Physical Chemistry. *J. Chem. Educ.* 2005, 82(2), pp. 241, <https://doi.org/10.1021/ed082p241>
- [26] B.Meyer. Elemental sulfur. *Chem. Rev.* 1976, 76(3), p. 367-388, <https://doi.org/10.1021/cr60301a003>